Technical Note N-1331

THE COANDA-EFFECT OIL-WATER SEPARATOR: A FEASIBILITY STUDY

BY

D. Pal

February 1974

Sponsored by

Director of Navy Laboratories

Approved for public release; distribution unlimited.

Civil Engineering Laboratory
Naval Construction Battalion Center
Port Hueneme, CA 93043

UNCLASSIFIED

SECURITY CLASSIFICATION OF THIS PAGE (When Data Entered)

REPORT DOCUMENTATION PAGE		READ INSTRUCTIONS BEFORE COMPLETING FORM
1. REPORT NUMBER TN-1331	2. GOVT ACCESSION NO.	3. RECIPIENT'S CATALOG NUMBER
4. TITLE (and Subtitle) The Coanda-Effect Oil-Water Separator: A Feasibility Study		5. TYPE OF REPORT & PERIOD COVERED Not final 6. PERFORMING ORG. REPORT NUMBER
7. AUTHOR(s) D. Pal		8. CONTRACT OR GRANT NUMBER(s)
9. PERFORMING ORGANIZATION NAME AND ADDRESS CIVIL ENGINEERING LABORATORY Naval Construction Battalion Center Port Hueneme, California 93043		10. PROGRAM ELEMENT, PROJECT, TASK AREA & WORK UNIT NUMBERS ZF61-512-001-058
11. CONTROLLING OFFICE NAME AND ADDRESS		12. REPORT DATE February 1974 13. NUMBER OF PAGES 42
14. MONITORING AGENCY NAME & ADDRESS(if different from Controlling Office) Director of Navy Laboratories Washington, D.C. 20376		15. SECURITY CLASS. (of this report) UNCLASSIFIED 15a. DECLASSIFICATION/DOWNGRADING SCHEDULE

16. DISTRIBUTION STATEMENT (of this Report)

Approved for public release; distribution unlimited.

17. DISTRIBUTION STATEMENT (of the abstract entered in Block 20, if different from Report)

18. SUPPLEMENTARY NOTES

19. KEY WORDS (Continue on reverse side if necessary and identify by block number)

Oil-water separator	Gravitation
Coanda effect	Coalescence
Effluent	Ultrafiltration
Centrifugation	Laminar flow

20. ABSTRACT (Continue on reverse side if necessary and identify by block number)

An experimental investigation which establishes the feasibility of using the Coanda-effect in developing an oil-water separator is described. Tests conducted on an experimental model with an oil-water mixture containing 6% oil showed that the oil content in the effluent can be reduced to less than 3%. A three-stage separator has produced effluent in the range of 1%. Conceptual designs of a practical separator are discussed. The space

DD FORM 1 JAN 73 1473 EDITION OF 1 NOV 65 IS OBSOLETE

UNCLASSIFIED

SECURITY CLASSIFICATION OF THIS PAGE (When Data Entered)

20. Continued.

requirement for a Coanda-effect separator when compared with typical parallel-plate type separators of the same capacity is considerably smaller. Analytical expressions useful in designing a Coanda-effect separator of a given size are also given.

INTRODUCTION

The Navy is faced with very strict regulations covering the discharge of oily wastes from its ships and shore facilities. Such wastes primarily originate from ship's bilges and ballast waters, oil spill recovery operations, fuel storage and transfer systems, and garage and maintenance activities. Technology and hardware are being developed to process such wastes so that effluent will meet EPA requirements.

Current methods of separating oil from oil-water mixtures are centrifugation, gravitation, coalescence and ultrafiltration [1,2]. Centrifugation is an accepted method for separating water-oil dispersions or emulsions [2]. Commercial equipment is available for a wide range of applications. Despite their effectiveness, the power requirement, cost and maintenance of such systems is relatively high. The gravitation method of separating oil from oily wastes relies upon differences in densities of the fluids being separated. Commercially available API and Heil type parallel separators are based upon the gravitation principle. Because of the laminar flow requirements for separation such systems are normally bulky. Coalescence has been used quite extensively for removing finely dispersed water droplets from fuels. The basic mechanism behind this separation technique is the formation of larger oil drops on the coalescing material. The resulting larger drops are separated by gravity. The method, however suffers from fouling of the coalescing element and requires frequent maintenance. Finally, ultrafiltration uses a filtering process to separate water from oil. This method, although very effective, suffers from fouling of the filter element. The system requires frequent cleaning.

A new method of separating free oil from oil-water mixtures [3] is under investigation at the Naval Civil Engineering Laboratory* (NCEL). This technique uses the fluid dynamic phenomenon, called ''wall attachment, or Coanda effect'', named after its discoverer, Henry Coanda. This effect is seen, for example, when one's finger is held close to a thin stream of water issuing from a tap or when tea is poured from a badly designed teapot-spout.

A preliminary investigation was conducted to establish the feasibility of using the Coanda effect for separating two immiscible liquids. This report describes in detail the feasibility program.

*On 1 January 1974 redesignated the Civil Engineering Laboratory (CEL) of the Naval Construction Battalion Center, Port Hueneme, California.

THEORY

Consider a thin jet sheet, quasi-two-dimensional, flowing into an unbounded region. The jet gets deflected towards an adjacent wall. When such wall is relatively close to the jet axis, the jet gets attached to and flows along the wall enclosing a separation bubble as shown in Figure 1. As is evident, the jet undergoes considerable curving during its attachment thus generating a centrifugal force field on it. This results in a lower pressure within the separation bubble. The pressure p_B in the separation bubble as derived in Appendix A is given by

$$P_\infty - p_B = J/b_o \frac{3\theta}{\sigma(1/t_1^2 - 1)} \tag{1}$$

where

P_∞ = free stream pressure,
J = jet momentum per unit span of the nozzle,
b_o = nozzle width,
θ = angular location of the reattachment point,
σ = jet spread parameter,
t_1 = $\tanh\left[\sigma y_1/(s_1 + s_o)\right]$
s_1 = axial distance between the reattachment point and the nozzle,
y_1 = half width of the jet at the reattachment point,
s_o = $\sigma b_o/3$ = distance of the nozzle exit from a hypothetical origin of the jet.

Using the theory discussed in Appendix A, dimensionless pressure $(P_\infty - p_B)\, b_o/J$ was plotted against the plate offset D/b_o for values of 7.7, 10 and 12 for the jet spread parameter σ. Figure 2 shows the pressure difference between the separation bubble and the ambient as a function of D/b_o.

For a jet composed of a mixture of two fluids which do not mix such as oil and water, the lighter fluid flowing along the plate side of the jet seeks the separation bubble and gets trapped by it. If an outlet is provided at the center of the bubble, the accumulated oil can be tapped out while the water and rest of the oil flows out of the device. This is the principle of operation of the Coanda-effect oil-water separator.

EXPERIMENTAL PROGRAM

A test program was designed to determine the feasibility of

using the wall-attachment effect in separating two liquids. Two experimental elements with different flow parameters were built and tested. The experiments were conducted in the Mechanical Systems Laboratory at NCEL using a mixture of regular tap water and hydraulic oil as the test fluid.

The Wall Attachment Elements

Based upon the theory developed in Appendix A, two experimental elements, namely, Elements No. 1 and No. 2 were designed. The 12-inch-long attachment wall of each element has an offset of 4 inches. The nozzles on Elements No. 1 and No. 2 are 1/4 and 3/8 inches wide respectively. The depth of flow passages on both elements is 1/4 inch. Element No. 1 was designed to carry 0.8 gpm of water flow whereas Element No. 2 has a flow carrying capacity of 1.5 gpm. The jet flow parameters such as reattaching distance x_R, jet center line radius r and its half width y_o at the reattachment point were determined from Figures A-2 through A-5 given in Appendix A. The jet spread parameter, σ, for the above calculations was chosen to be 12. The dimensions of the elements are listed in Table 1.

Each element consisted of three major components: top and bottom cover plates, and the middle plate with the flow passages machined in it. For ease of fabrication and to facilitate flow visualization during tests, each component plate of the Elements was made of transparent plexi-glass sheet. Further, to extract the accumulated oil in the separation bubble, a 1/4 inch diameter outlet was provided in the top cover plate of each element. The general layout showing major dimensions of the elements is given in Figure 3. The elements were assembled by gluing the two cover plates to the middle plate.

Feasibility Tests

The experiments were performed using the test setup shown in Figure 4. The adjustment of supply water flow is possible by hand controlled valves provided on the flow line. A mixture of red hydraulic oil (Appendix B) and water was used as the test-fluid. The mixture was formed by injecting the oil into water stream before it entered the element. To form a homogenous mixture, the oil was released at the center of and parallel to the water flow in the pipe. The oil to the mixing junction was supplied by a variable flow pump (see details in Appendix B). The element was immersed in water throughout the test series. The supply water flow was measured by a rotameter. The static pressure in the water line was measured by conventional pressure gauges. The use of red oil in the test mixture allowed flow visualization through the elements. The photographs of flow patterns were taken by mounting a camera directly above the elements.

The feasibility tests were conducted by running the oil

Table 1. Parameters of the Test Elements

Parameter	Element No. 1	Element No. 2
Nozzle width, b_o, inches	1/4	3/8
Wall offset, D, inches	4.0	4.0
Attachment wall length, ℓ, inches	12.0	12.0
Radius, D/b_o	16.00	10.67
Flow passage depth, h, inches	1/4	1/4
Designed water flow, gpm	0.80	1.50
Velocity at the nozzle at designed flow, feet/second	4.10	5.13
Reynold's number* at the nozzle, at designed flow	7119.7	13354.7
Jet Momentum at the nozzle, J lbs/ft	0.6794	1.595
Preducted pressure, p_B, within the separation bubble (from Figure 2) inches of H_2O	0.1978	0.3935
Predicted Attachment distance, x_R (from Figure A-5) inches	6.6	7.2
Predicted Jet center-line radius, r (from Figure A-4) inches	7.75	9.0
Predicted half width of the jet, y (from Figure A-3) inches	0.251	0.345

*Kinematic viscosity of water at 60 degrees F taken as 1.2×10^{-5} ft^2/second.

water mixture containing 6 to 8% oil by volume through the elements. The optimum water flow rates were 0.8 gpm through Element No. 1 and 1.5 gpm through Element No. 2 respectively. The mixture jet reattachment distances from the corners were measured for both elements. They were found to be 7 inches for Element No. 1 and 7.5 inches for No. 2. These values are very close to the theoretically computed values listed in Table 1. The test results indicated that a portion of the oil in the mixture jet did accumulate in the separation bubble zone of the flow. A photograph of the flow pattern (Figure 5) through Element No. 2 at its optimum flow rate clearly shows the accumulation of oil in the separation bubble. This oil when extracted contained about 50% water. Consequently, improved designs for collecting oil transferred into the separation bubble were sought. One such design is that of providing a chamber at the top of the separation bubble. This chamber is connected to the separation bubble by means of holes in the top cover plate of the element, see Figure 6. Under optimum conditions, the oil captured by the separation bubble flows into the collecting chamber through the connecting holes. Next, the oil collected in the chamber is transferred by siphoning to an oil storage tank. Two different designs of the collecting chambers were tested. These are shown in Figures 7 and 8. Due to its shape and its greater depth, the collecting chamber design shown in Figure 8 is more efficient in collecting the oil. Tests conducted on the elements with modified design show that about 50% of the oil in the input flow can be extracted in this manner, whereas the remaining oil flows out with the attached water jet. Furthermore, the oil being extracted contained about 5% water. Thus, a separating device based upon this concept appears to be capable of gross separation only. However, tests on elements with modified designs must be conducted before deriving final conclusions about the degree of separation obtainable. A photograph of the flow pattern through the Element No. 1 taken at its optimum flow rate is included as Figure 9. The accumulation of oil in the collecting chamber is clearly visible in this record.

Tests On A Multi-Stage Element

It was realized during the feasibility tests on the single-stage elements that to make the Coanda-effect separator suitable for practical applications, staging is necessary. The number of stages for the separator, however, depends upon the type of oily wastes being handled together with the quality of effluent desired.

During the course of this study a three-stage test element was designed and built to evaluate the effect of staging. Figure 10 shows the sketch of the element's middle plate with flow passages cut in it. Each stage of the element has a 1/4 inch

wide nozzle. The depth of element's flow passage was kept at 1/4 inch. The mixture jet in each stage is directed by a curved wall conforming to the curvature of a reattaching jet issuing parallel to a flat plate with an offset of 4 inches. This boundary was determined from flow governing equations given in Appendix A. The element was designed to handle 0.8 gpm of water flow through each stage. Each stage was provided with oil collecting chambers located directly on its separation bubble zone. The oil outlet line on each oil chamber was provided with a hand controlled valve for outgoing oil flow adjustment.

The element was tested using the setup shown in Figure 4. The tests were conducted by varying the oil in the mixture from 6 to 8%. The test results indicate that each stage separated about 50% of the oil from its input flow. The effluent at the third stage outlet contained about 1% oil. The oil being extracted had about 3 to 5% water. Figure 11 shows the element undergoing tests. The flow pattern through the element is shown in Figure 12. The accumulation of oil in the collecting chambers and the separated oil flowing through the outflow lines are shown in the flow record.

DISCUSSION

Jet Velocity Distribution

As mentioned earlier, the mixture jet during its attachment, develops a centrifugal acceleration. It was assumed prior to conducting the tests that the lateral acceleration so induced would force most of the oil in the jet into the separation bubble zone of the flow. The observed flow patterns through the experimental models on the other hand revealed that the oil particles were distributed uniformly over the entire cross-section of the jet. This important observation can be explained from theoretical considerations discussed in Appendix A.

Consider the reattaching jet velocity profile described by Equation 2:

$$u(s,y) = \left[\frac{3J\sigma}{4\rho(s+s_o)}\right]^{\frac{1}{2}} \, \mathrm{Sech}^2 \; \frac{\sigma y}{s+s_o} \qquad (2)$$

where the various symbols are defined in Appendix A. The width of a two-dimensional jet expanding into a similar fluid at any axial location can be derived easily from a linear relationship given in References 4 and 5. The half width, y_1 of the jet is given by

$$y_1 = \left(\frac{s+s_o}{s_o}\right) b_o/2 \qquad (3)$$

It can be seen from Equation 2 that the jet velocity u(s,y) is maximum at its center-line and is

$$umax = \left[\frac{3J\sigma}{4\rho(s+s_o)}\right]^{\frac{1}{2}} \qquad (4)$$

Next, it can be deduced from Equations 2 and 3 that the jet velocity u(s,y) drops to 0.1814 umax at a distance equal to the half width of the jet from its center line. The centrifugal acceleration distribution in the jet can be derived from Equation 2 and is given by

$$\ddot{u}(s,y) = \frac{3J\sigma}{4\rho(s+s_o)(r\pm y)} \operatorname{sech}^4 \frac{\sigma y}{s+s_o} \qquad (5)$$

Again it is evident from Equation 4 that the centrifugal acceleration, u(s,y) is maximum at the jet center line and is

$$\ddot{u}max = \frac{3J\sigma}{4\rho(s+s_o)r} \qquad (6)$$

The acceleration drops sharply to approximately 0.0327 umax at the jet half-width points.

The typical velocity and acceleration for the reattaching jets are shown in Figure 13. Because of the nature of lateral acceleration on the jet, the oil particles are distributed over the entire cross-section. Such a distribution of centrifugal acceleration affects the separating capability of a separator with this configuration.

The mixture jet velocity and hence its centrifugal acceleration distribution can be improved by modified designs. One such design is shown in Figure 14. The device uses a splitter located at the nozzle center-line to divide the mixture jet into two sub-jets which flow along the curved walls as shown. The mixture jets flowing through the device will have velocity distribution as shown in the figure, i.e., from a maximum near the curved

walls monotonically decreasing to zero at the separation bubble center. Such a velocity distribution will induce a monotonically decreasing centrifugal acceleration on the jet with a maximum near the wall. This configuration will force most of the oil into the separation bubble. The effluent flows out through the two outlets provided on the device. Such a design should improve the separating capabilities of the separator markedly. An experimental investigation is underway to evaluate this concept.

Another possible improvement in the oil separation capability of the device can be accomplished by decreasing the static pressure within the separation bubble of the flow. This can be achieved by increasing the centrifugal force on the mixture jet which in turn can be increased by decreasing the radius of the jet center-line. The separation bubble pressure can also be decreased by increasing jet efflux momentum.

An Automated Oil Extraction System

It was observed during the feasibility tests that the rate of oil extraction from the oil collecting chambers of the elements affected the quality of oil being extracted appreciably. Too high an extraction rate disturbed the oil-water interface in the collecting chamber and the oil being extracted contained up to 50% water. A low oil extraction rate on the other hand reduced the rate of oil captured by the separation bubble of the flow. This resulted in more oil in the effluents thereby deteriorating the performance of the device. A system to control the oil extraction rate is, therefore, required for proper functioning of the separator. Such a system can be either a proportional or on-off type. Because of the simplicity of their design and their lower costs, systems of the on-off type are considered for this application.

One such system, shown in Figure 15, uses the difference in electrical conductance of water and that of the oil. Practically all oils are electrical insulators. Water (excluding pure water) is capable of conducting electricity. The system of Figure 15 uses this property in sensing the oil-water interface in the collecting chamber by providing two electrodes at different heights in it. For sensing, the electrodes are connected to a 10 volt AC supply through a 1000 ohm resistor. The solenoid valve on the outgoing oil line is operated by the output of the amplifier which receives its input from a rectified voltage signal across the resistor in the sensing circuit. The use of AC supply in the sensing circuit minimizes the electrolysis in the collecting chamber. When the oil-water interface is below the bottom electrode, the resistance in the sensing circuit is very high and practically no current flows through it.

This configuration leads to opening of the solenoid valve provided on the oil outlet line. As the oil is extracted the oil-water interface in the chamber eventually rises above the bottom electrode thereby decreasing the resistance in the sensing circuit. This results in a voltage across the resistor, which when amplified closes the solenoid valve and thus stops the oil extraction. The feasibility of the system will be determined by testing it on the experimental model of the separator.

Alternative means of sensing the oil-water interface may be employed in the foregoing control system. Use of an ultrasonic transducer, although expensive, can sense the oil-water interface precisely. Another means of sensing which can be used is based upon the photo-electric principle. Irrespective of the type of sensing used, the basic design of the control system remains unchanged.

COMPARISON WITH THE TYPICAL PARALLEL PLATE SEPARATORS

It was learned from the feasibility tests that a separating device based upon the Coanda-effect principle is capable of gross separation only. Therefore, for an evaluation the separator should be compared with typical, laminar flow parallel plate separators.

Because of its design configuration and the flow velocities through it, the Coanda-effect separator will have a considerably smaller physical size. For instance, a separator to treat 20 gpm of oil-water flow rate can be 1.5 feet long x 1 foot wide x 1.5 feet high; whereas typical parallel plate type separator [1] of the same flow capacity occupies 3 feet--3-1/2 inches x 3 feet--6 inches x 1 foot 7 inches of space. The physical size comparison of the Coanda-effect separators with typical parallel plate type separators for handling 20 and 100 fpm of mixture flow rates is given in Table 2. Because of its smaller size, for a given flow rate, the equipment cost of the Coanda-effect separator will be lower.

Presently, the Coanda-effect separator is in its early stages of development and thus many design modifications are required, therefore, a comparison of its oil separating capabilities with that of the fully developed parallel plate separator is not possible. More work is required before such a comparison can be made. Finally, because of the simplicity of its design, the maintenance of the separator promises to be easier.

Table 2. Physical Size Comparison of the Coanda Effect and Typical Parallel Plate Separators

No.	Maximum Designed Mixture Flow Through the Separator	Coanda-Effect Separator	Parallel Plate Separator
1	20 gpm	1 foot-6 inches long, 1 foot wide, and 1 foot 6 inches high	3 feet-3-1/2 inches long, 3 feet-6 inches wide, and 1 foot-7 in inches high
2	100 gpm	3 feet long, 2 feet wide, and 1 foot-6 inches high	5 feet-9 inches long, 3 feet-6 inches wide, and 3 feet-2 inches high

CONCLUSIONS AND RECOMMENDATIONS

1. The investigation conducted to date establishes the feasibility of using the Coanda effect principle in developing an oil-water separator. A separator based upon this concept will be considerably smaller than a laminar-flow separator of comparable capacity.

2. Feasibility tests conducted on an experimental model of the separator, with an oil-water mixture containing 6% oil (mixture flow rate of 1.5 gpm), show that the oil content can be reduced to less than 3%. The extracted oil contained only 5% water. To make the separator practical, staging is necessary.

3. Further, to improve the quality of extracted oil, an automated oil extraction rate controlling system is required. A concept of one such system given should be investigated by testing it on the experimental separator.

4. Improvements in the separating effectiveness of the separator can be accomplished by modifying the velocity distribution of the mixture jet to alter the centrifugal acceleration on it. A conceptual design of such a modification has been formulated.

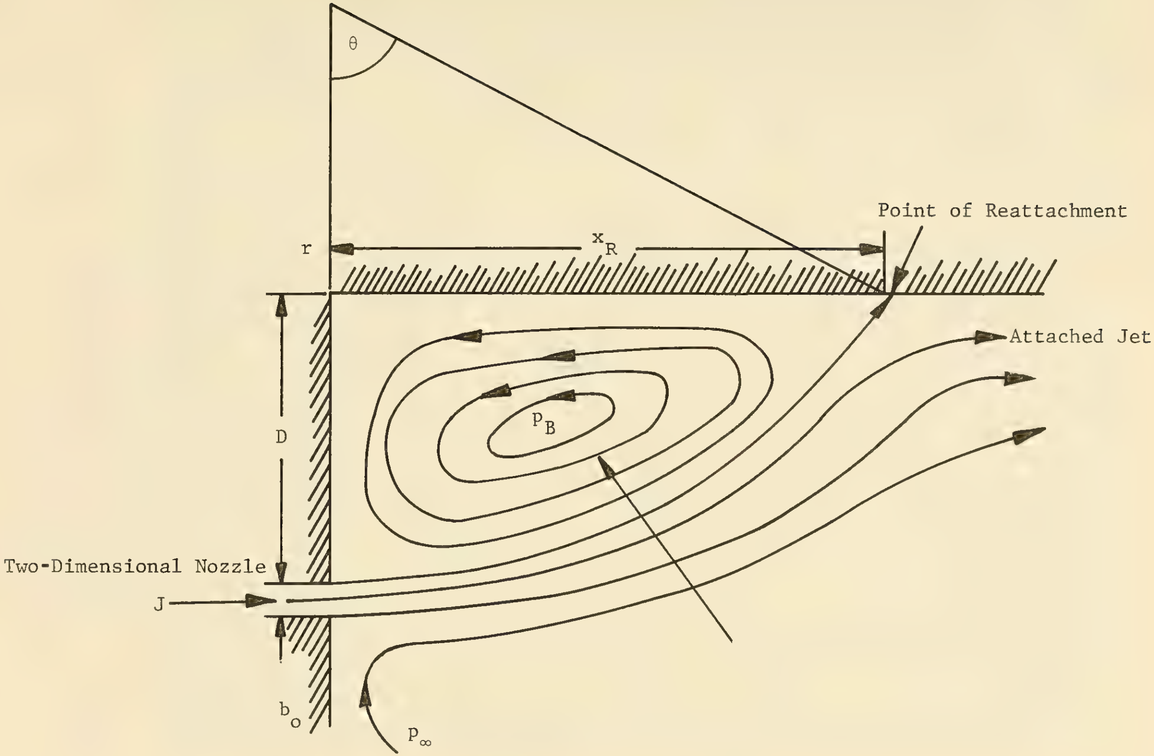

Figure 1. Two-Dimensional Jet Attaching to an Offset Parallel Plate

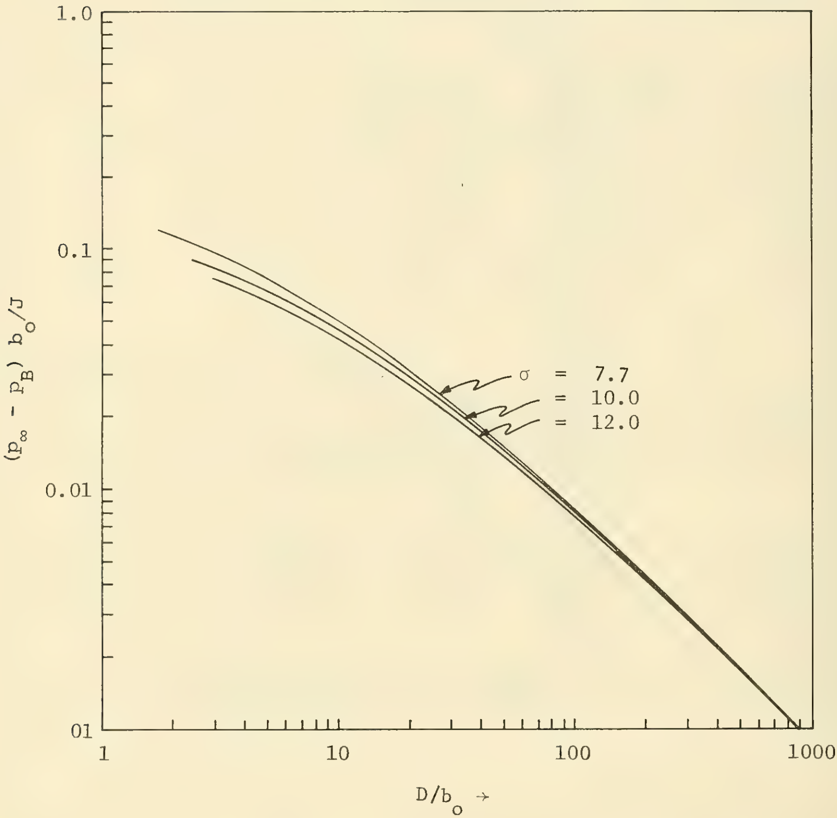

Figure 2. Dimensionless pressure $(p_\infty - p_B)b_o/J$ plotted against plate offset parameter D/b_o for various values of σ of 7.7, 10 and 12.

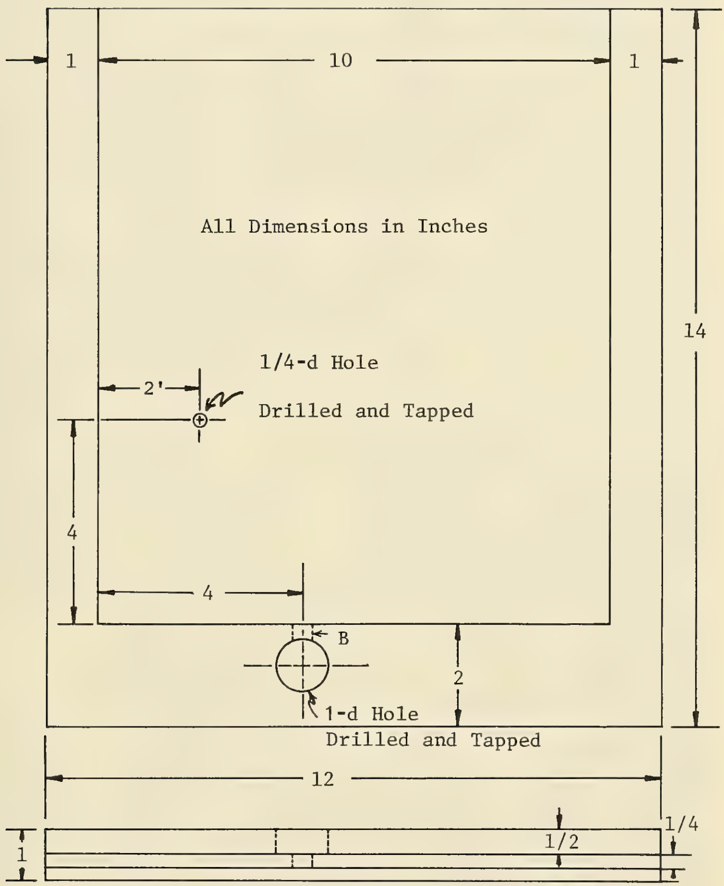

B is 1/4 inch for Element No. 1

B is 3/8 inch for Element No. 2

Figure 3. Sketch of the Test Element.

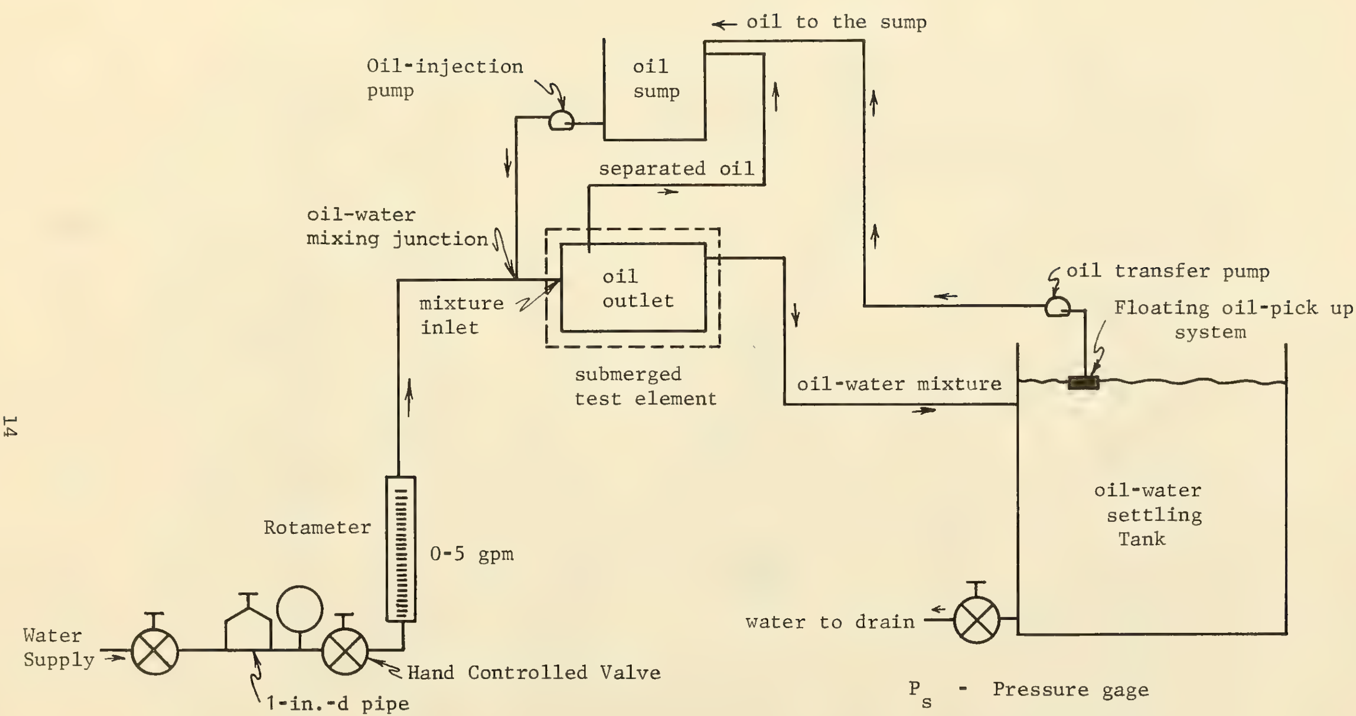

Figure 4. Schematic of the Test Setup.

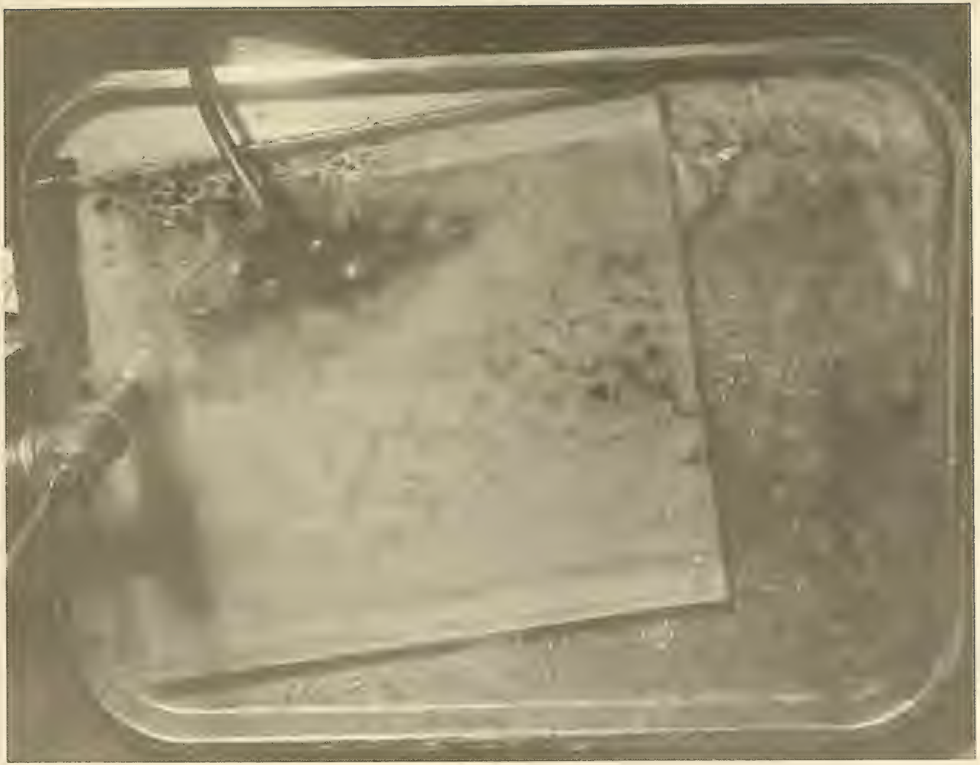

Figure 5. Flow pattern through Element No. 2 at a mixture flow rate of 1.5 gpm water with 7% oil.

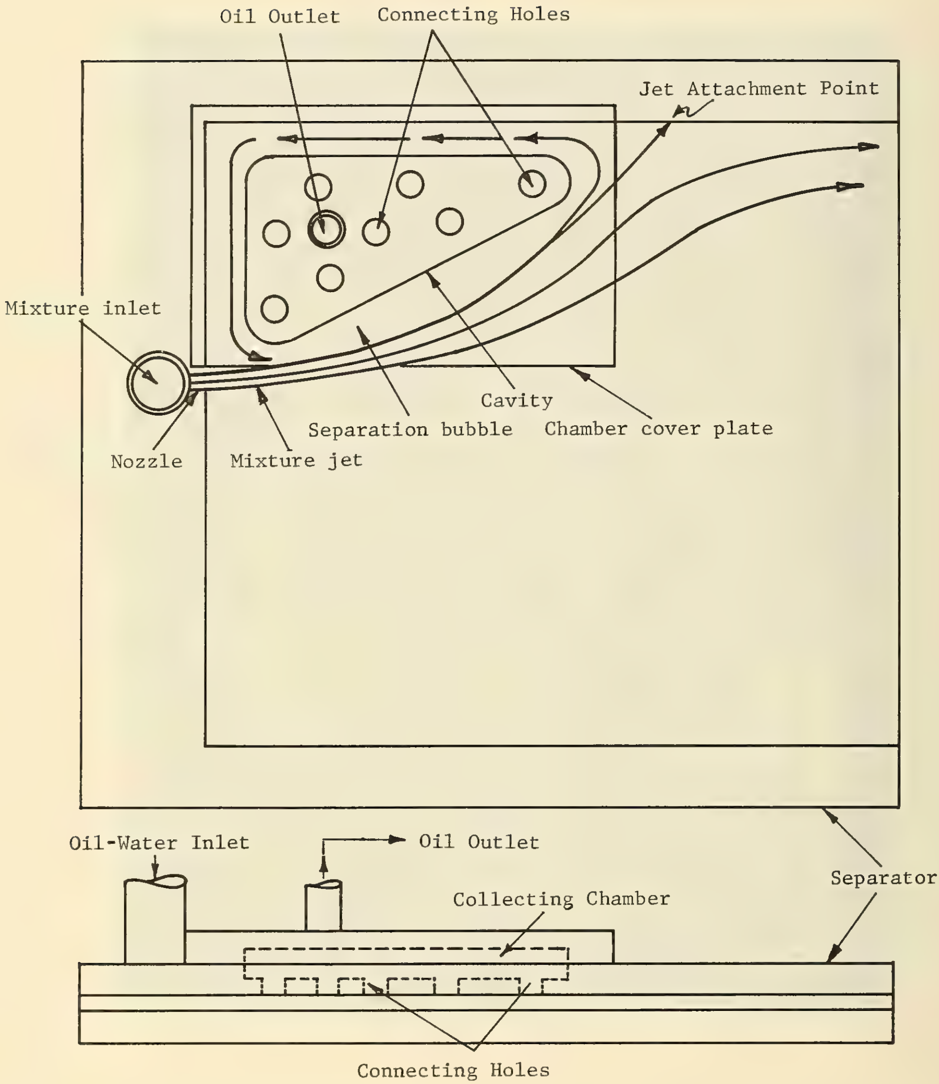

Figure 6. Single Stage Coanda Effect Oil-Water Separator Test Model.

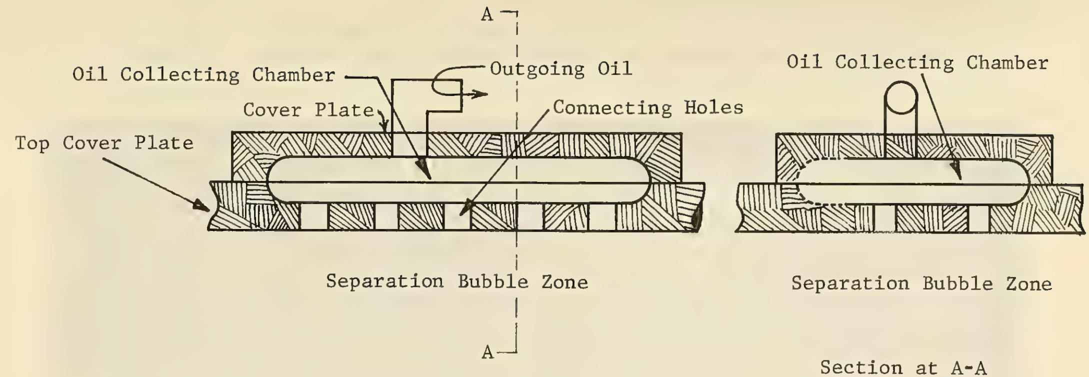

Figure 7. Design features of the oil collecting chamber.

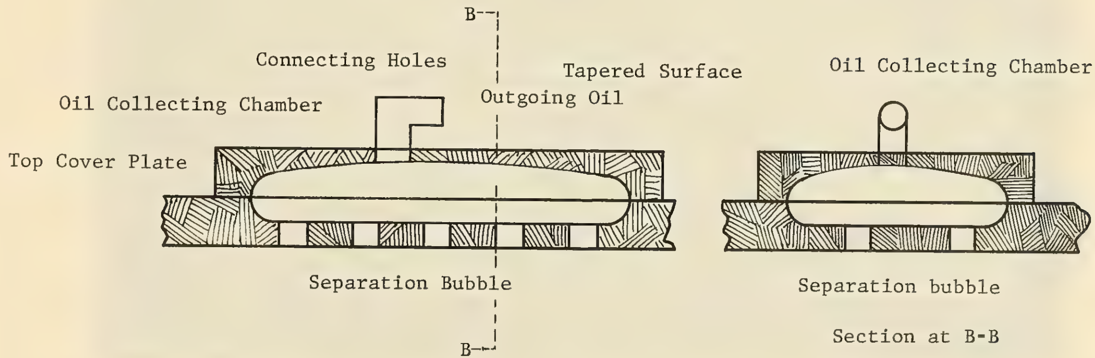

Figure 8. Modified design of the oil collecting chamber.

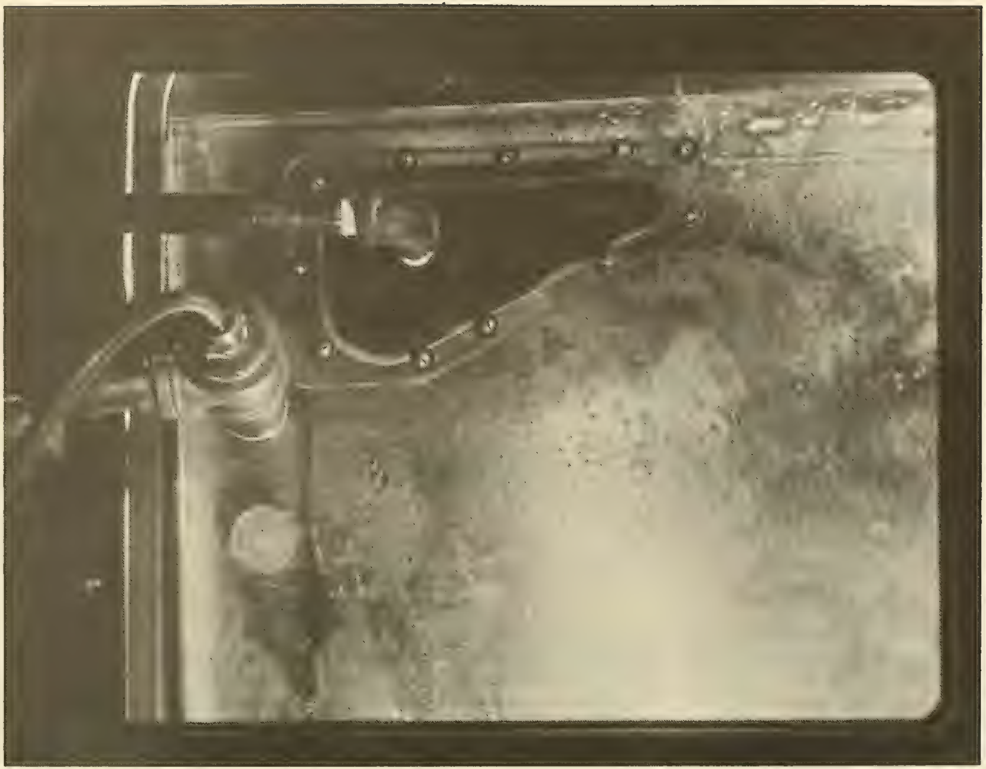

Figure 9. Flow pattern through the modified element no. 1 at 0.8 gpm water flow rate with 6% oil.

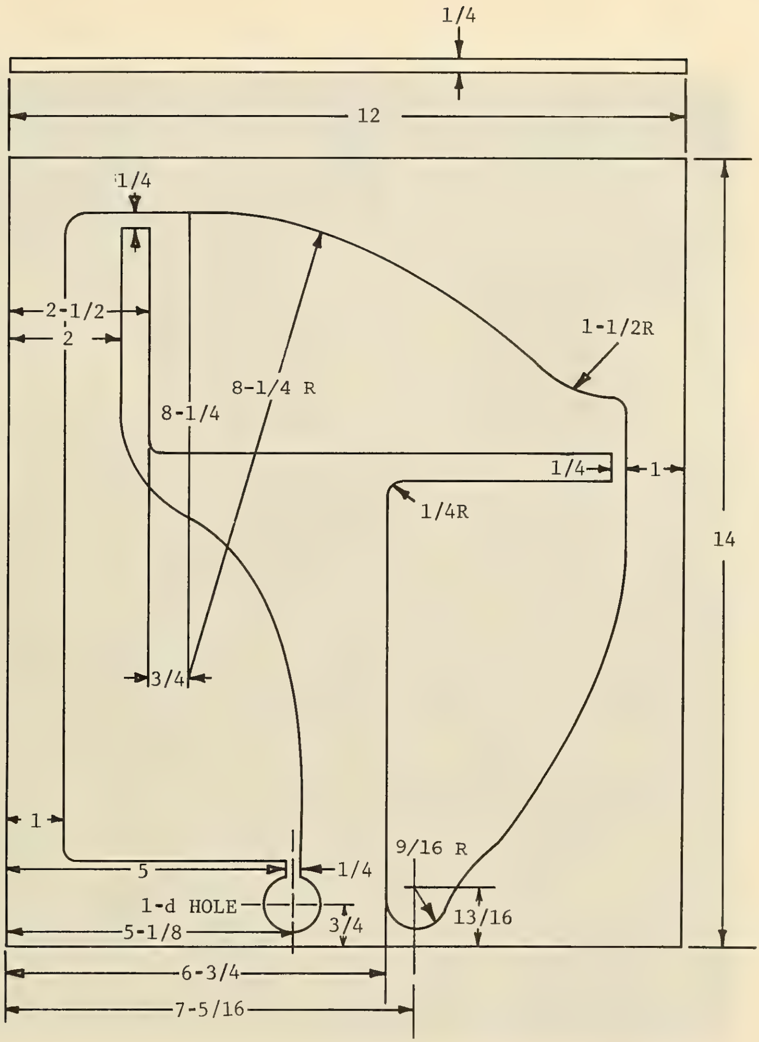

All Dimensions in Inches

Figure 10. The Sketch of Experimental 3-Stage Element

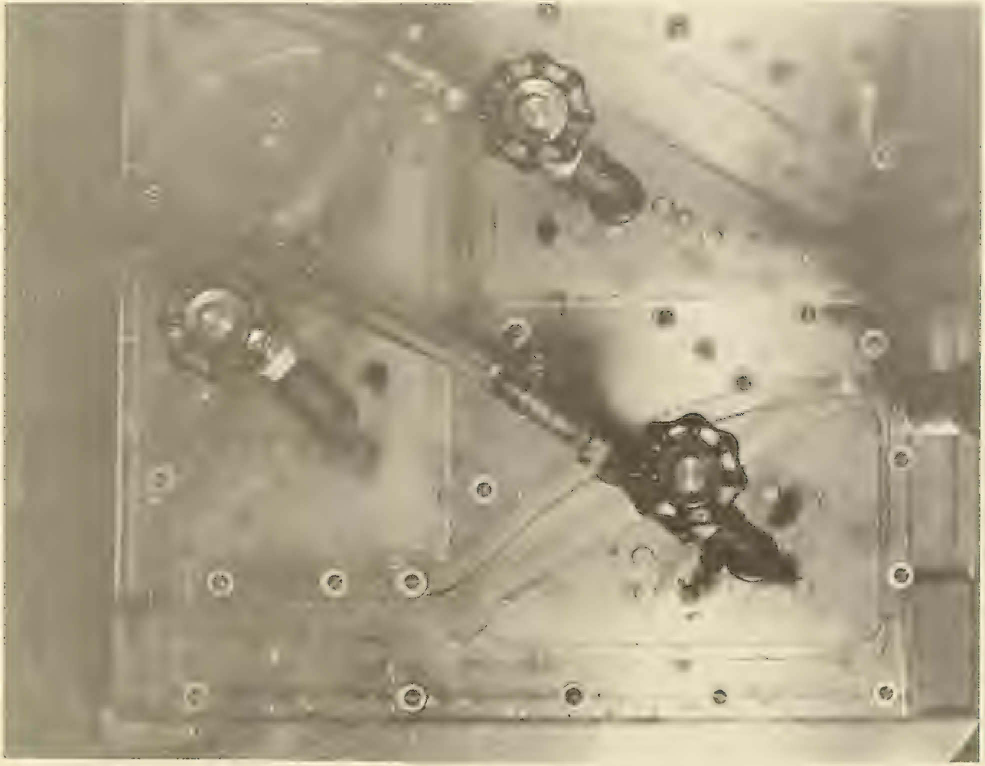

Figure 11. The three-stage test element with water flow only. The flow through device is 0.9 gpm. (The oil droplets in the collecting chambers is the residual oil from the previous tests.)

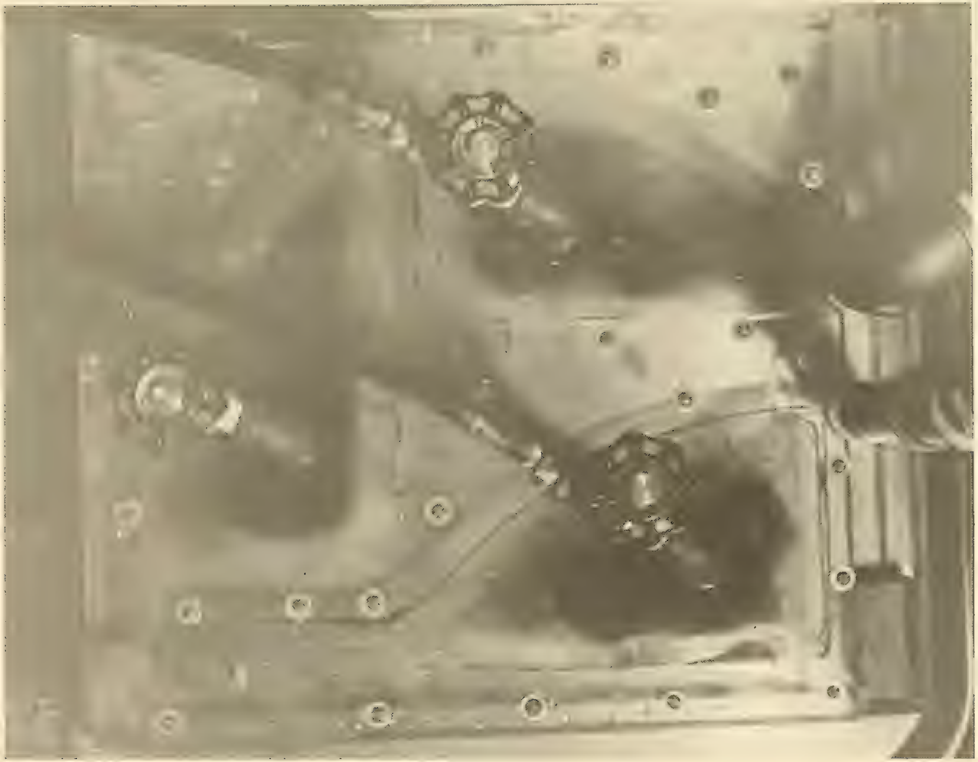

Figure 12. Flow pattern through the three stage repainting device at 0.9 gpm water flow with 6% oil.

$$u_{max} = \left[\frac{3J\sigma}{4\rho(s+s_o)} \right]^{\frac{1}{2}} \qquad u_{max} = \frac{3J\sigma}{4\rho(s+s_o)r}$$

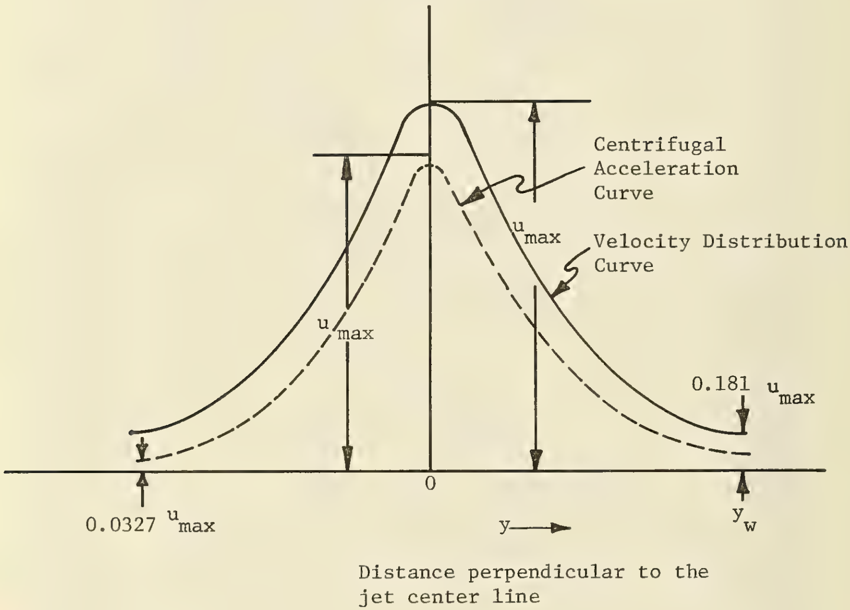

Figure 13. Reattaching Jet Axial Velocity and Centrifugal Acceleration Distributions

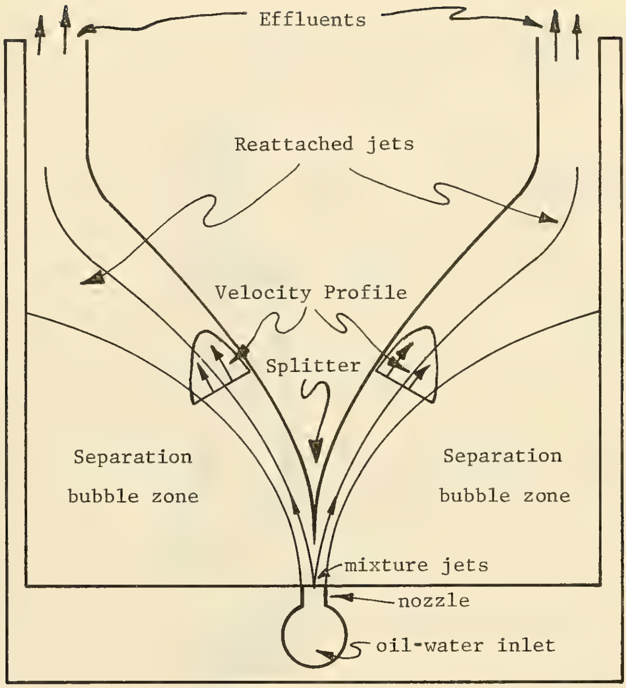

Figure 14. Conceptual Design of a Modified Separator with Improved Jet Velocity Profiles.

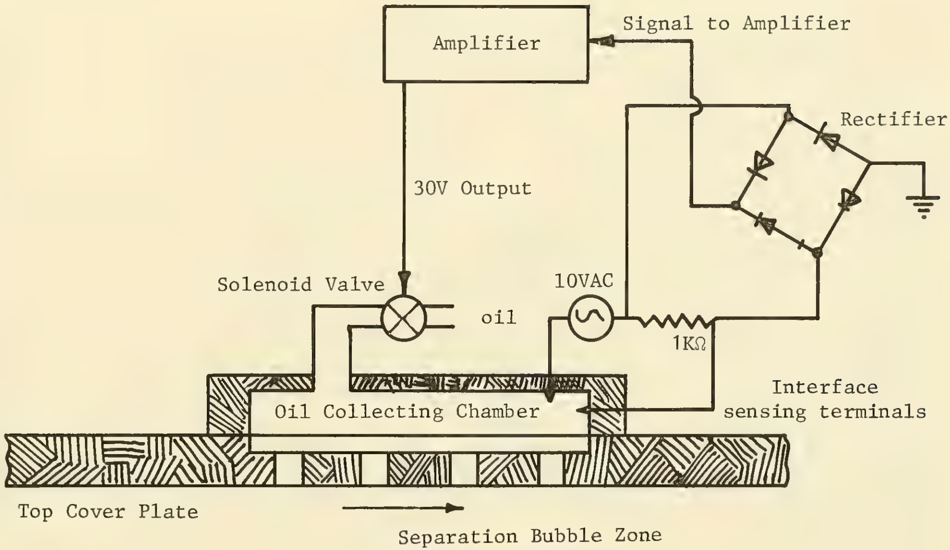

Figure 15. Schematic of an Oil Extraction System

Appendix A

EQUATIONS AND DATA DESCRIBING THE FLOW RESULTING FROM A TWO-DIMENSIONAL INCOMPRESSIBLE JET ISSUING PARALLEL TO AN OFFSET FLAT PLATE.

This appendix lists the equations and data describing the flow resulting from a two dimensional incompressible jet issuing parallel to an offset flat plate.

Wall Attachment Flow Analysis

This problem has been treated in depth by Bourque and Newman [4], and by Sawyer [5] independently. The analysis conducted by Bourque and Newman is easier to understand and covers a wide range of flow parameters. In this study therefore only the results of Reference 4 were used.

The analysis can be described by considering the flow of a two-dimensional jet issuing from a nozzle in a wall adjacent to a parallel plate with an offset D as shown in Figure A-1. The jet during its expansion entrains fluid from the surroundings by turbulent action. The entrainment of fluid from the plate side causes a pressure difference across the jet thus curving it toward the plate. If the plate is sufficiently long the jet strikes it and reattaches. The jet divides on striking the plate, sending part of the flow into the separation bubble. The flow equibilibrium is reached when the flow entrained by the plate side of the jet is equal to that into the separation bubble from the jet at the point of striking. This is the model used in the analysis of Reference 4. Further, the analysis is based upon the following assumptions:

(1) The flow is incompressible and two dimensional, i.e., only thin jet sheets are considered.

(2) The jet efflux velocity is uniform, i.e., the increase in its velocity with the reduced pressure in the separation bubble is neglected. The jet is submerged in a similar fluid and its velocity distribution is that of a free jet.

(3) The jet entrains the same amount of fluid from each boundary.

(4) Pressure within the separation bubble is constant and the jet center line is a circular arc up to the point of attachment.

(5) The force on the plate due to skin friction forces are small and are neglected.

The axial component of jet velocity used is

$$u(s,y) = \left[\frac{3J\sigma}{4\rho(s+s_o)}\right]^{\frac{1}{2}} \text{Sech}^2 \frac{\sigma y}{s+s_o} \qquad (2)$$

where

s = axial distance from the nozzle,
b_o = nozzle width,
s_o = distance of the nozzle from a hypothetical origin of the jet where the flow originates,
y = co-ordinate normal to the jet center line,
σ = jet spread parameter, to be determined experimentally, it has a value of 7.7 for a turbulent free jet,
s_o = $\sigma b_o/3$ (see Reference 4).

Before going any further some quantities must be defined as follows:

P_∞ = free stream pressure
p_B = Static pressure within the separation bubble
r = radius of the center line of the reattached jet,
ρ = density of the fluid,
θ = Angular location of the point of reattachment from the nozzle,
D = distance of the plate from the nozzle axis,
x_R = distance of the point of attachment from the corner,
ℓ = length of the plate
J = jet momentum per unit span of the nozzle.

The equation of the reattaching streamline is given by

$$\frac{3s}{\sigma b_o} = (1/t^2)-1 \qquad \text{(A-1)}$$

$$\text{where } t = \tanh \frac{\sigma y}{s + s_o} \qquad \text{(A-2)}$$

$$\text{if } t = t_1 \qquad \text{(A-3)}$$

$$\text{where } t_1 = \tanh \frac{\sigma y_1}{s_1+s_o} \tag{A-4}$$

is the value of t at the point of reattachment, then the radius of the jet center line is derived from

$$r/b_o = \frac{\sigma(1/t_1^2 - 1)}{3\theta} \tag{A-5}$$

where t_1 and θ are determined from the following equations:

$$D/b_o = \frac{\sigma(1/t_1^2 - 1)(1 - \text{Cos}\ \theta)}{3\theta} - \frac{1}{2} \tag{A-6}$$

and

$$\text{Cos}\ \theta = 3/2\ t_1 - 1/2\ t_1^3 \tag{A-7}$$

The half width of the jet at the reattachment point, i.e., y, can be easily derived from Equation A-4 and is

$$y_1/b_o = 1/3t_1^2\ \tanh^{-1} t_1 \tag{A-8}$$

Further, the distance of the reattachment point from the plane of the nozzle is

$$x_R/b_o = \frac{\sigma(1/t_1^2 - 1)\ \text{Sin}\ \theta}{3\theta} - \frac{\tanh^{-1} t_1}{3t_1^2\ \text{Sin}\ \theta} \tag{A-9}$$

Finally, the mean pressure within the separation bubble is computed by

$$p_\infty - p_B = J/b_o \left[\frac{3\theta}{\sigma(1/t_1^2 - 1)}\right] \tag{A-10}$$

A wall attachment element can be designed using Equations (A-1) through (A-9).

However, to use these equations conveniently, it is required that the flow parameters x_R/b_o, r/b_o, y_1/b_o and θ be known as functions of the pre-determined parameter D/b_o. These equations are complex and can not be expressed explicitly in terms of D/b_o alone.

A numerical scheme was devised to compute x_R/b_o, r/b_o, y_1/b_o for known values of D/b_o. The numerical method runs as follows. By inspection of Equation A-7, maximum and minimum values of t_1 which render θ between 90 degrees and 30 degrees were determined. Since y_1 is positive, only positive values of r_1 must be considered. Further, it was determined from Equation A-7 that for θ to lie between 90 degrees and 30 degrees, t_1 must range between 0 and 0.50. A known value of t_1 yields θ from Equation A-7. For a selected value of σ with known t_1 and θ, parameters D/b_o, r/b_o, y_1/b_o and x_R/b_o can be determined from Equations A-6, A-5, A-8 and A-10 respectively. Thus computing a set of values for x_R/b_o r/b_o and y_1/b_o for a known D/b_o. A series of similar sets were computed by increasing t_1 by 0.05 each time up to a final value of 0.50. A total of three series of sets were computed for different θ of 12, 10 and 7.7 respectively.

For easy usage the parameters θ, y_1/b_o, r/b_o and x_R/b_o were plotted against D/b_o for values of D/b_o ranging from 1 to 1000. These plots are shown in Figures A-2 through A-5. It should be added here that flow parameters become independent of the parameter D/b_o for D/b_o greater than 35. Also the analysis becomes inaccurate for D/b_o less than 3. Further, the value of σ, , the spread parameter chosen can affect the flow parameters appreciably.

One last remark of interest is regarding the value of σ, the spread parameter to be used while using these curves. Because of the curvature effect a σ of 7.7 does not apply. It is reported in Reference 1 that a value of 12 for σ gives flow parameters values that are in fair agreement with the experimental data.

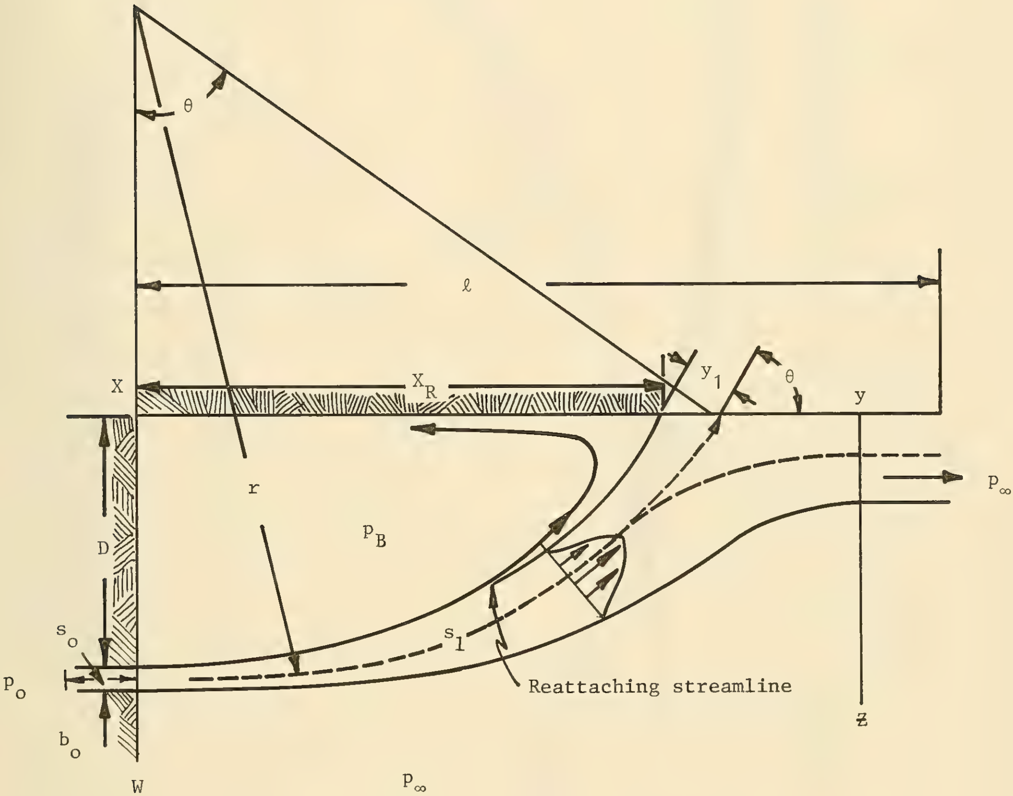

Figure A-1. A two-dimensional jet reattached to an offset parallel plate.

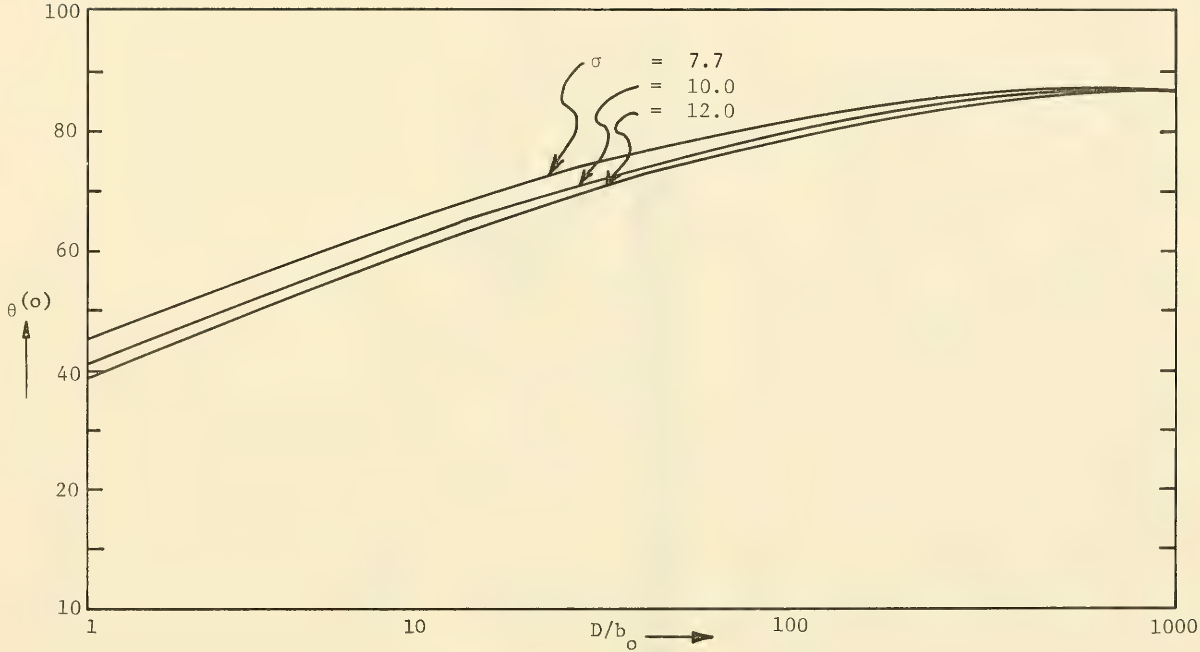

Figure A-2. Angular location (θ) of the jet reattachment point plotted against plate offset parameter D/b_o for various values of σ of 7.7, 10 and 12.

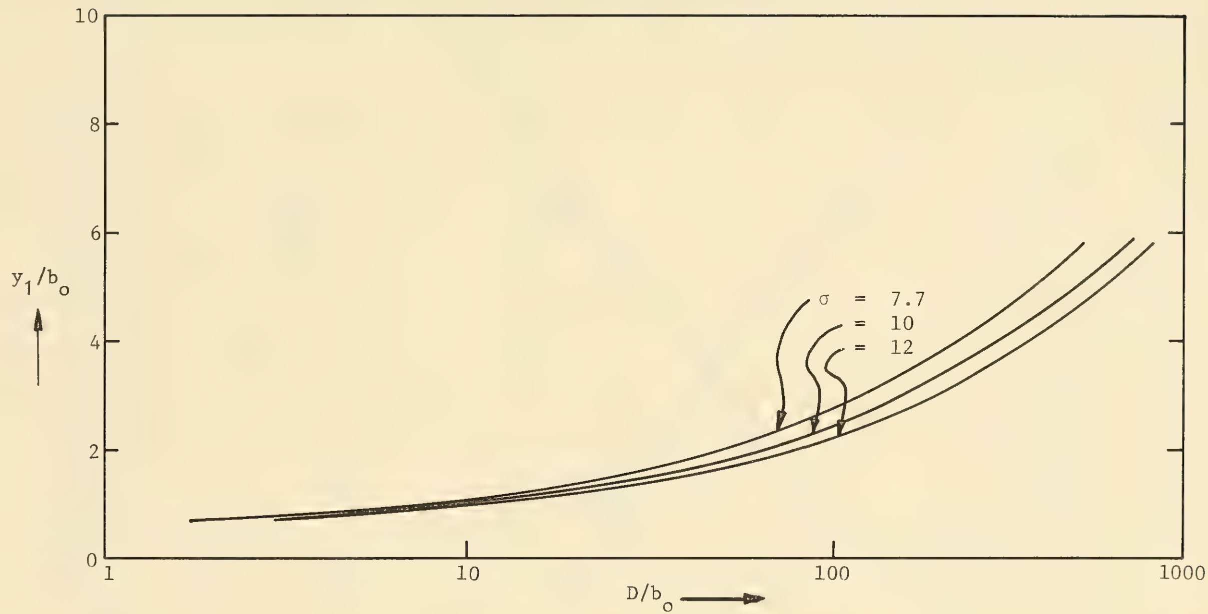

Figure A-3. Half-width (y_1/b_o) of the jet at the reattachment point plotted against plate offset parameter D/b_o for various values of σ of 7.7, 10 and 12.

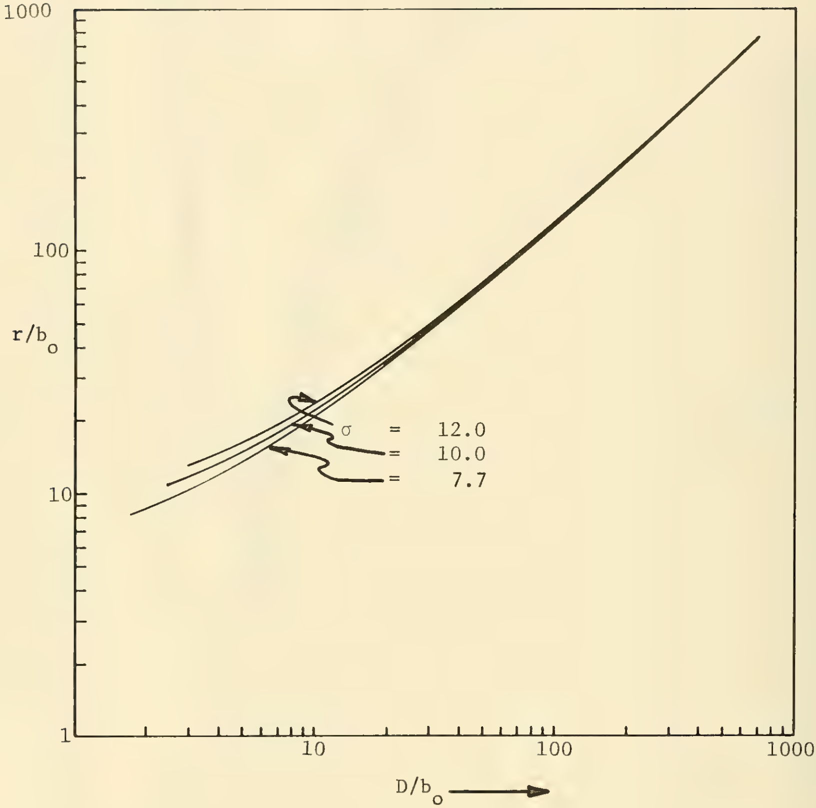

Figure A-4. Jet center line radius r/b_o plotted against plate offset D/b_o for various values of σ of 7.7, 10 and 12.

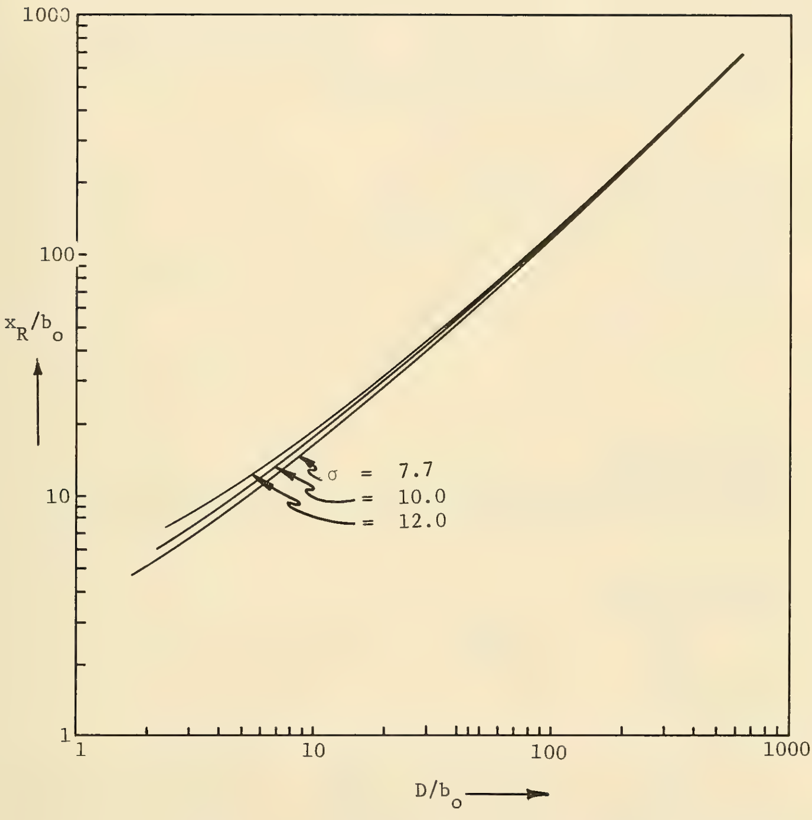

Figure A-5. Reattachment distance x_R/b_o plotted against plate offset for various values of σ of 7.7, 10 and 12.

Appendix B

SPECIFICATIONS OF OIL USED IN THE TEST MIXTURE AND THE OIL INSPECTION PUMP

This appendix lists the specification of
(a) the oil used in the test mixture
(b) the oil inspection pump

Hydraulic Fluid - Petroleum Base
Mil. spec.: MIL-H-5606C
Fed. Stock No.: FSN 9150-223-4134
Specific gravity: 0.88 to 0.90
Color: red
Kinematic viscosity: 8.0 stokes at 40 degrees F
to 0.10 stokes at 130 degrees F

Oil Injection Pump

Fluid Metering Corp
FMI Model RRP-F
with 3/8-inch piston, 0-100 cc/min at 50 psi. Variable flow with micrometer flow adjustment head. Electric motor drive. 115V, 4.5A at 60 cycles, 1725 rpm.

ACKNOWLEDGMENTS

John B. Curry assisted in the laboratory tests of the experimental elements

REFERENCES

1. Naval Civil Engineering Laboratory. Mechanical and electrical engineering department, letter report, YF38.554.001.01.001: Program plan for oily waste handling at navy shore establishment, by E.L. Ghormley, Ph.D., Port Hueneme, California, June 1972.
2. S.M. Finger and R.B. Tabakin, Development of shipboard oil/water separation systems, ASME paper 73-ENAS-38, presented at the intersociety conference on Environmental Systems, San Diego, California, July 16-19, 1973.
3. U.S. Navy Case 56,734: Patent application on coanda effect oil-water separator, by A.J. Paszyc, Ph.D., D. Pal and J.B. Curry, 15 June 1973.

4. C. Bourque and B.G. Newman, Reattachment of a two-dimensional imcompressible jet to an adjacent flat pole, the Aeronautical Quarterly, Vol XI, Aug, 1960, pp. 201-232.
5. R.A. Sawyer, The flow due to a two dimensional jet issuing parallel to a flat plate, J. Fluid Mech. Vol 9, 1960, pp. 543-60.
6. Naval Civil Engineering Laboratory. Contract Report CR 73.015: Test and evaluation of oil-water separation systems by the Ben Holt Co., Pasadena, California, Port Hueneme, California, 8 Nov. 1972.

DISTRIBUTION LIST

SNDL Code	No. of Activities	Total Copies	
--	1	12	Defense Documentation Center
--	1	1	Director of Navy Laboratories
FKAIC	1	3	Naval Facilities Engineering Command
FKN1	6	6	NAVFAC Engineering Field Divisions
FKN5	9	9	Public Works Centers
FA25	1	1	Public Works Center
--	9	9	RDT&E Liaison Officers at NAVFAC Engineering Field Divisions and Construction Battalion Centers
--	298	298	CEL Special Distribution List No. 8 for persons and activities interested in reports on Mechanical Systems

Natick Labs*
Kansas St.
Natick, MA 01761

Public Works Officer
Boston Naval Shipyard
Boston, MA 02129

Public Works Officer
Naval Hospital, Boston
Chelsea, MA 02150

Dr. E. M. Lenoe
Army Materials & Mechanics Research Center
Bldg 39, Room 412
Arsenal Street
Watertown, MA 02172

Public Works Officer
Naval Air Station
South Weymouth, MA 02190

LCDR David A. Cacchione, USN
Office of Naval Research, Broff
495 Summer Street
Boston, MA 02210

Public Works Officer
Naval Facility
Nantucket, MA 02554

Public Works Officer
Naval Air Station
Quonset Point, RI 02819

Commanding Officer (Code 200)
Navy Public Works Center
Naval Base
Newport, RI 02840

Commanding Officer
Naval Supply Depot
Newport, RI 02840

President
Naval War College
Code 22
Newport, RI 02840

Commanding Officer
U.S. Naval Station
Naval Base
Newport, RI 02840

Staff Civil Engineer
Naval Supply Center
Newport, RI 02840

Mr. S. Milligan
SB 322
Naval Underwater Systems Center
Newport, RI 02844

Public Works Officer
Naval Underwater Systems Center
Newport, RI 02844

Commanding Officer
CBC Technical Library
Naval Construction Battalion Center
Davisville, RI 02854 (2 copies)

Public Works Officer
Portsmouth Naval Shipyard
Portsmouth, NH 03801

Public Works Officer
U.S. Naval Disciplinary Command
Portsmouth, NH 03801

Public Works Officer
Naval Air Station
Brunswick, ME 04011

Public Works Officer
Naval Radio Station (T), Cutler
East Machias, ME 04630

Facilities Officer
Code NA 2
New London Laboratory
Naval Underwater Systems Center
New London, CT 06320

Public Works Department
Box 400
Naval Submarine Base, New London
Groton, CT 06340

Commanding General
U. S. Army Electronics Command
Attn: AMSEL-GG-TD
Fort Monmouth, NJ 07703

Public Works Officer
Naval Air Propulsion Test Center
Trenton, NJ 08628

* All addressees receive one copy unless otherwise indicated.

Public Works Officer
Naval Air Station
Lakehurst, NJ 08733

Commanding Officer
Mobile Construction Battalion 74
FPO New York 09501

Public Works Officer
U. S. Naval Support Force Antarctica
FPO New York 09501

Commanding Officer
Amphibious Construction Battalion TWO
FPO New York 09501

Public Works Officer
U.S. Naval Activities, United Kingdom
FPO New York 09510

Public Works Officer
U.S. Naval Activities, United Kingdom Det.
FPO New York 09510

Public Works Officer
U. S. Naval Communication Station
FPO New York 09512

Public Works Officer
U. S. Naval Security Group Activity
FPO New York 09518

Public Works Officer
U. S. Naval Air Facility
FPO New York 09520

Public Works Officer
U.S. Naval Support Activity
FPO New York 09521

Director
European Branch-Atlantic Division
Naval Facilities Engineering Command
Naval Support Activity-Box 51
FPO New York 09521

Public Works Officer
U. S. Naval Air Facility
FPO New York 09523

Public Works Officer
U. S. Naval Communication Station
FPO New York 09525

Public Works Officer
U.S. Naval Control of Shipping Office
FPO New York 09526

Public Works Officer
U. S. Naval Medical Research Unit No. 3
FPO New York 09527

Public Works Officer
U.S. Navy Fleet Support Office
FPO New York 09532

LT Ronald A. Milner, CEC, USN
U. S. Naval Station
Box 9
FPO New York 09540

Public Works Officer
Morocco-U. S. Naval Training Command
Box 19
FPO New York 09544

Public Works Officer
U. S. Naval Communication Station
Box 41
FPO New York 09544

Public Works Officer
U.S. Navy Support Activity
FPO New York 09550

Public Works Officer
U.S. Naval Station
FPO New York 09551

Commanding Officer
U.S. Naval Hospital
FPO New York 09551

Public Works Officer
U. S. Naval Facility
FPO New York 09552

Public Works Officer
U. S. Naval Facility
FPO New York 09553

Public Works Officer
U.S. Naval Communication Station
FPO New York 09554

Public Works Officer
U.S. Naval Security Group Activity
FPO New York 09555

Public Works Officer
U. S. Naval Facility
FPO New York 09558

Public Works Officer
U. S. Naval Air Station
FPO New York 09560

Public Works Officer
U. S. Naval Station
FPO New York 09571

Public Works Officer
U. S. Naval Communication Station
FPO New York 09580

Public Works Officer
U. S. Naval Support Activity
FPO New York 09585

Public Works Officer
U. S. Naval Station
Box 25
FPO New York 09593

Public Works Officer
U. S. Naval Station
Box 6
FPO New York 09597

Public Works Officer
U. S. Naval Communication Station
APO New York 09843

Public Works Officer, Naval Station
136 Flushing Avenue
Brooklyn, NY 11251

Public Works Officer
Naval Strategic Systems Navigation Facility
Flushing & Washington Avenue
Brooklyn, NY 11251

Public Works Officer
U. S. Naval Hospital
St. Albans, LI, NY 11425

Public Works Officer
Naval Ships Parts Control Center
Mechanicsburg, PA 17055

Public Works Officer
Naval Air Development Center
Warminster, PA 18974

Public Works Officer
Naval Air Station
Willow Grove, PA 19090

Commanding Officer
Code 016A
Northern Division
Naval Facilities Engineering Command
Philadelphia, PA 19112

RDT&E Liaison Officer
Code 102 Northern Division
Naval Facilities Engineering Command
Philadelphia, PA 19112

Public Works Officer
Philadelphia Naval Shipyard
Philadelphia, PA 19112

Commanding Officer
Naval Station
Philadelphia, PA 19112

Public Works Officer
Naval Air Engineering Center
Philadelphia, PA 19112

Public Works Officer
Naval Hospital
17th Street & Pattison Avenue
Philadelphia, PA 19145

Public Works Officer
National Naval Medical Center
Bethesda, MD 20014

Mr. R. B. Allnutt
Code 1706
Naval Ship Research & Development Center
Bethesda, MD 20034

Head Facilities & Industrial Department
Code 54
Carderock Laboratory
Naval Ship Research & Development Center
Bethesda, MD 20034

William F. Gerhold
National Bureau of Standards
Corrosion Section
Washington, DC 20234

Chief of Engineers
U. S. Army
DAEN-MCE-D
Washington, DC 20314

Commander
Naval Ship Systems Command
Code OOC
Washington, DC 20362

Mr. David L. Southey
Code 41A
Bureau of Medicine and Surgery
Navy Department
Washington, DC 20372

U.S. Naval Oceanographic Office
Library - Code 3600
Washington, DC 20373

Director
Naval Research Laboratory
Code 2627
Washington, DC 20375

Public Works Officer
Naval Research Laboratory
4555 Overlook Ave., SW
Washington, DC 20375

Director of Navy Laboratories
Room 300, Crystal Plaza Bldg 5
Department of the Navy
Washington, DC 20376

Commanding Officer
Chesapeake Division - Code 03
Naval Facilities Engineering Command
Washington Navy Yard
Washington, DC 20390

Director, Design Division - 04
Chesapeake Division
Naval Facilities Engineering Command
Washington Navy Yard
Washington, DC 20390

Public Works Officer
Naval Air Facility
Washington, DC 20390

Commandant
Naval District Washington
Public Works Department - Code 412
Washington, DC 20390

Public Works Officer
Naval Security Station
3801 Nebraska Avenue, NW
Washington, DC 20390

Public Works Officer
Naval Communication Station
Washington, DC 20390

Mr. M. R. Whitley
Criteria & Research Branch
Office of Construction Management
General Services Administration
Washington, DC 20405

Commanding Officer
Naval Explosive Ordnance
Disposal Facility - Code TI 1
Indian Head, MD 20640

Public Works Officer
Naval Ordnance Station
Indian Head, MD 20640

Public Works Officer
Naval Air Station
Patuxent River, MD 20670

Commander
Naval Ship Engineering Center
Code 6136
Prince Georges Center
Hyattsville, MD 20782

Commander
Naval Ship Engineering Center
Code 6162
Prince Georges Center
Hyattsville, MD 20782

Technical Library
Naval Ship Engineering Center
622 Center Bldg
Prince Georges Center
Hyattsville, MD 20782

Chief
Marine & Earth Sciences Library
National Oceanic & Atmospheric Admin.
Dept of Commerce
Rockville, MD 20852

M. E. Ringenbach
Engineering Development Lab (C61)
National Oceanic & Atmospheric Admin.
National Ocean Survey
Rockville, MD 20852

Public Works Officer
Naval Ordnance Laboratory, White Oak
Code 942
Silver Spring, MD 20910

Commanding Officer
ATTN: STEAP-TL
Bldg 305
Aberdeen Proving Ground, MD 21005

Director
Division of Engineering & Weapons
U. S. Naval Academy
Annapolis, MD 21402

Dr. Neil T. Monney
Naval Systems Engineering Dept
U. S. Naval Academy
Annapolis, MD 21402

Public Works Department
U. S. Naval Academy
Annapolis, MD 21402

Library, Code 5642
Annapolis Laboratory
Naval Ship Research & Dev. Center
Annapolis, MD 21402

Public Works Officer
Naval Support Facility
Box 277
Thurmont, MD 21788

U.S. Army Coastal Eng. Research Center
Kingman Building
Fort Belvoir, VA 22060

Public Works Officer
Marine Corps Dev. Education Command
Quantico, VA 22134

Facilities Officer
Office of Naval Research
Code 108
800 North Quincy Street
Arlington, VA 22217

Dr Nicholas Perrone
Code 439
Office of Naval Research
800 North Quincy Street
Arlington, VA 22217

Oceanographer of the Navy
ATTN: Code N712
200 Stovall Street
Alexandria, VA 22332

CAPT Pharo A. Phelps, CEC, USN
Naval Facilities Engineering Command
200 Stovall Street
Alexandria, VA 22332

Commander
Code 0436B
Naval Facilities Engineering Command
200 Stovall Street
Alexandria, VA 22332

Public Works Officer
Naval Weapons Laboratory
Dahlgren, VA 22448

Public Works Officer
Fleet Combat Direction Systems
Training Center, Atlantic
Dam Neck
Virginia Beach, VA 23461

Public Works Officer
Naval Weapons Station
Yorktown, VA 23491

Commanding Officer
Navy Public Works Center
Norfolk, VA 23511

Staff Civil Engineer
Naval Air Station
Norfolk, VA 23511

RDT&E Liaison Officer
Code 09P2
Atlantic Division
Naval Facilities Engineering Command
Norfolk, VA 23511 (2 copies)

Director
Amphibious Warfare Board
Naval Amphibious Base, Little Creek
Norfolk, VA 23521

Public Works Officer
Naval Amphibious Base, Little Creek
Norfolk, VA 23521

General Engineer
Naval Hospital
Portsmouth, VA 23708

Director
Engineering Division - Code 440
Public Works Department
Norfolk Naval Shipyard
Portsmouth, VA 23709

Public Works Officer
Naval Facility, Cape Hatteras
Buxton, NC 27920

Public Works Officer
Marine Corps Air Station
Cherry Point, NC 28533

Public Works Officer
Marine Corps Air Station, New River
Jacksonville, NC 28540

Public Works Officer
Marine Corps Base
Camp Lejuene, NC 28542

Public Works Officer
Charleston Naval Shipyard
Naval Base
Charleston, SC 29408

Staff Civil Engineer
Naval Hospital
Charleston, SC 29408

Public Works Officer
Naval Station
Naval Base
Charleston, SC 29408

RDT&E Liaison Officer
Southern Division - Code 90
Naval Facilities Engineering Command
P. O. Box 10068
Charleston, SC 29411

Staff Civil Engineer
Naval Supply Center
Charleston, SC 29411

Public Works Officer
Naval Hospital
Beaufort, SC 29902

Public Works Officer
Marine Corps Air Station
Beaufort, SC 29902

Public Works Officer
P. O. Box 35
Marine Corps Recruit Depot
Parris Island, SC 29905

Public Works Officer
Naval Air Station, Atlanta
Marietta, GA 30063

Public Works Officer
Navy Supply Corps School
Athens, GA 30601

Public Works Department
Naval Air Station
Glynco, GA 31520

Public Works Officer
Naval Air Station
Albany, GA 31703

Public Works Officer
Marine Corps Supply Center
Albany, GA 31704

Director of Engineering
Naval Air Station
Jacksonville, FL 32212

Public Works Officer
Naval Air Station
Cecil Field, FL 32215

AFCEC/DE
Tyndall Air Force Base, FL 32401

R. E. Elliott
Code 710
Naval Coastal Systems Laboratory
Panama City, FL 32401

Public Works Officer
Naval Coastal Systems Laboratory
Panama City, FL 32401

Staff Civil Engineer
Naval Air Station
Pensacola, FL 32508

Commanding Officer (Code 200)
Navy Public Works Center, Bldg 1
Naval Air Station
Pensacola, FL 32508

Public Works Officer
Naval Air Station, Whiting Field
Milton, FL 32570

Public Works Officer
Naval Training Center
Orlando, FL 32813

Staff Civil Engineer
Naval Training Equipment Center
Orlando, FL 32813

Public Works Officer
Naval Security Group Activity
Homestead, FL 33030

Public Works Officer
Naval Station
Key West, FL 33040

Staff Civil Engineer
Naval Air Station
Key West, FL 33040

Public Works Officer
Naval Air Station, Memphis (84)
Millington, TN 38054

Staff Civil Engineer
Naval Hospital Memphis
Millington, TN 38054

Public Works Officer
Naval Air Station
Meridian, MS 39301

Public Works Officer
Naval Ordnance Station
Louisville, KY 40214

AFIT
Civil Engineering School
Wright-Patterson AFB, OH 45433

Public Works Officer
Naval Avionics Facility
Indianapolis, IN 46218

Public Works Officer
Naval Ammunition Depot
Crane, IN 47522

Public Works Officer
Naval Air Facility, Detroit
Mount Clements, MI 48043

Public Works Officer
Naval Air Station
Glenview, IL 60026

Army Construction Eng. Research Lab.
ATTN: Library
P. O. Box 4005
Champaign, IL 61820

Commanding Officer - Engineering Div.
MRD-Corps of Engineers
Department of the Army
P. O. Box 103, Downtown Station
Omaha, NE 68101

Public Works Department
Maintenance Division
Naval Air Station, New Orleans
Belle Chasse, LA 70037

Public Works Officer
Naval Air Station, New Orleans
Belle Chasse, LA 70037

Public Works Officer
Naval Ammunition Depot
McAlester, OK 74501

Public Works Officer
Naval Air Station
Dallas, TX 75211

Public Works Officer
Naval Air Station
Chase Field
Beeville, TX 78102

Public Works Officer
Naval Air Station
Corpus Christi, TX 78419

Public Works Department
Marine Corps Air Station
Yuma, AZ 85364

Technical Reference Division
Headquarters, Fort Huachuca
Fort Huachuca, AZ 85613

AFWL
CE Division
Kirtland AFB, NM 87117

Public Works Officer
Naval Ordnance Missile Test Facility
White Sands Missile Range, NM 88002

Public Works Officer
Naval Air Station
Fallon, NV 89406

Public Works Officer
Naval Ammunition Depot
Hawthorne, NV 89415

Public Works Officer
Naval Air Station
Los Alamitos, CA 90720

Public Works Officer
Naval Weapons Station
Seal Beach, CA 90740

Public Works Officer
Naval Station
Long Beach, CA 90801

Dr Arthur R. Laufer
Office of Naval Research, BROFF
1030 East Green Street
Pasadena, CA 91106

Officer in Charge
Pasadena Laboratory - Naval Undersea Center
ATTN: Technical Library
3202 E. Foothill Blvd
Pasadena, CA 91107

Asst. Public Works Officer
Naval Weapons Station
Fallbrook Annex
Fallbrook, CA 92028

Staff Civil Engineer
Naval Air Station
Imperial Beach, CA 92032

Public Works Officer
Marine Corps Base
Camp Pendleton, CA 92055

Dr J. D. Stachiw
Code 6505
Naval Undersea Center
San Diego, CA 92132

Mr. R. E. Jones
Code 65402
Naval Undersea Center
San Diego, CA 92132

Technical Library
Code 1311
Naval Undersea Center
San Diego, CA 92132

Public Works Officer
Code 75
Naval Undersea Center
San Diego, CA 92132

Staff Civil Engineer
Naval Training Center
San Diego, CA 92133

Public Works Officer
Naval Administrative Command
Naval Training Center
San Diego, CA 92133

Civil Staff Engineer
Naval Hospital
San Diego, CA 92134

Public Works Officer
Naval Air Station
North Island
San Diego, CA 92135

Staff Civil Engineer
Naval Station
San Diego, CA 92136

Commanding Officer
Navy Public Works Center
Naval Base
San Diego, CA 92136

Public Works Officer
Naval Air Station
Miramar
San Diego, CA 92145

Public Works Officer
Naval Amphibious Base
Coronado
San Diego, CA 92155

Public Works Officer
Naval Air Facility
El Centro, CA 92243

Public Works Officer
Marine Corps Base
Bldg 1130
Twentynine Palms, CA 92278

Public Works Officer
Marine Corps Supply Center
Barstow, CA 92311

Public Works Department (151)
Marine Corps Air Station
El Toro
Santa Ana, CA 92709

Commanding Officer
Naval Missile Center
Code 5632.2, Technical Library
Point Mugu, CA 93042

Office of Patent Counsel
Code PC (Box 40)
Naval Missile Center
Point Mugu, CA 93042

Public Works Officer
Naval Air Station
Point Mugu, CA 93042

Public Works Officer
Code 82
Naval Construction Battalion Center
Port Hueneme, CA 93043

Librarian, Code 9215
Construction Equipment Department
Naval Construction Battalion Center
Port Hueneme, CA 93043

Commander
31st Naval Construction Regiment
Naval Construction Battalion Center
Port Hueneme, CA 93043

Commanding Officer
Code 155
Naval Construction Battalion Center
Port Hueneme, CA 93043

Commanding Officer
Naval Schools of Construction
Port Hueneme, CA 93043

Public Works Officer (70)
Naval Weapons Center
China Lake, CA 93555

Public Works Officer
Naval Facility, Big Sur
Big Sur, CA 93920

Superintendent
Attn: Library (Code 2124)
Naval Postgraduate School
Monterey, CA 93940

Public Works Officer
Public Works Dept
Naval Postgraduate School
Monterey, CA 93940

Dr. Edward B. Thornton
Department of Oceanography
Naval Postgraduate School
Monterey, CA 93940

Public Works Officer
Naval Air Station
Moffett Field, CA 94035

Commanding Officer
Western Division - Code 09PA
Naval Facilities Engineering Command
P. O. Box 727
San Bruno, CA 94066

Commanding Officer
Western Division - Code 04
Naval Facilities Engineering Command
P. O. Box 727
San Bruno, CA 94066

Commanding Officer
Western Division - Code 04B
Naval Facilities Engineering Command
P. O. Box 727
San Bruno, CA 94066

Commanding Officer
Western Division - Code 05
Naval Facilities Engineering Command
P. O. Box 727
San Bruno, CA 94066

Commanding Officer
Western Division - Code 112
Naval Facilities Engineering Command
P. O. Box 727
San Bruno, CA 94066

Public Works Officer
Naval Station
Treasure Island
San Francisco, CA 94130

Asst. Resident OIC of Construction
Bldg 506
Hunters Point Naval Shipyard
San Francisco, CA 94135

Public Works Officer
San Francisco Bay Naval Shipyard
Hunters Point Division
San Francisco, CA 94135

Public Works Department (183)
Naval Air Station
Alameda, CA 94501

Public Works Officer
Mare Island Naval Shipyard
Vallejo, CA 94592

Asst. Public Works Officer
Naval Support Activity
Mare Island Naval Shipyard
Vallejo, CA 94592

Public Works Officer
Code 70
Naval Supply Center
Oakland, CA 94625

Public Works Officer
Naval Hospital
Oakland, CA 94627

Mr. H. Wheeler
Code 73.13
Naval Fuel Department
Point Molate
Richmond, CA 94804

Public Works Officer
Naval Communication Station San Francisco
Rough and Ready Island
Stockton, CA 95203

Public Works Officer
Naval Facility, Centerville Beach
Ferndale, CA 95536

Base Civil Engineer
Det 3, 15th ABW (PACAF)
APO San Francisco 96305

Director, Engineering Division
Officer in Charge of Construction
Naval Facilities Engineering Command
Contracts, Southwest Pacific
APO San Francisco 96528

Headquarters
Kwajalein Missile Range
Box 26, Attn: SSCR-RKL-C
APO San Francisco 96555

Commanding Officer
Mobile Construction FOUR
FPO San Francisco 96601

Commanding Officer
Mobile Construction Battalion TEN
FPO San Francisco 96601

Staff Civil Engineer
Pearl Harbor Naval Shipyard
Box 400
FPO San Francisco 96610

Staff Civil Engineer
Naval Supply Center
Box 300
FPO San Francisco 96610

Commander Pacific Division
Naval Facilities Engineering Command
FPO San Francisco 96610

RDT&E Liaison Officer
Pacific Division - Code 403
Naval Facilities Engineering Command
FPO San Francisco 96610

Mr. T. M. Ishibashi
Navy Public Works Center
Engineering Department - Code 200
FPO San Francisco 96610

Staff Civil Engineer
Naval Supply Center
Box 300
FPO San Francisco 96610

Public Works Officer
U.S. Naval Air Station
FPO San Francisco 96611

Public Works Officer
Engineering Division
Naval Ammunition Depot
FPO San Francisco 96612

Public Works Officer
U. S. Naval Station
Box 15
FPO San Francisco 96614

Mr. D. K. Moore
Hawaii Laboratory
Naval Undersea Center
FPO San Francisco 96615

Public Works Officer
U.S. Marine Corps Air Station
FPO San Francisco 96615

Staff Civil Engineer
U. S. Naval Communication Station
FPO San Francisco 96630

Staff Civil Engineer
U.S. Naval Station
FPO San Francisco 96630

Officer in Charge of Construction
Naval Facilities Engineering Command
Contracts, Marianas
FPO San Francisco 96630

Staff Civil Engineer
U.S. Naval Station
FPO San Francisco 96630

Technical Library
Engineering Department
U. S. Navy Public Works Center
Box 6
FPO San Francisco 96651

Staff Civil Engineer
U.S. Naval Station
FPO San Francisco 96651

Staff Civil Engineer
U.S. Naval Station
FPO San Francisco 96654

Asst. Public Works Officer
San Migual, Naval Communications Station
Box 1585
FPO San Francisco 96656

Public Works Officer
U.S. Naval Communication Station
FPO San Francisco 96680

Officer in Charge of Construction
Naval Facilities Engineering Command
Contracts
FPO San Francisco 96680

U.S. Naval Support Force Antarctica
Detachment 1
FPO San Francisco 96690

Public Works Officer
Naval Facility
Coos Head Empire Station
Coos Bay, OR 97420

Public Works Officer
Naval Support Activity
Seattle, WA 98115

Public Works Officer
Naval Air Station
Whiley Island
Oak Harbor, WA 98277

Public Works Dept., Code 400
Puget Sound Naval Shipyard
Bremerton, WA 98314

Public Works Officer
Naval Torpedo Station
Keyport, WA 98345

Commanding Officer
U.S. Navy Public Works Center
Box 13
FPO Seattle 98762

Commanding Officer
U. S. Naval Air Facility
Box 15
FPO Seattle 98767

Public Works Officer
U.S. Naval Security Group Activity
FPO Seattle 98768

Public Works Officer
Fleet Activities
FPO Seattle 98770

Public Works Officer
Marine Corps Air Station (H)
FPO Seattle 98772

Public Works Officer
Marine Corps Base
Camp Smedley D. Butler
FPO Seattle 98773

Public Works Officer
U. S. Naval Station
FPO Seattle 98791

Public Works Officer
U.S. Naval Communication Station
Box 30
FPO Seattle 98791

Colleges, etc.

Prof. W. E. Heronemus
Civil Engineering Dept.
University of Massachusetts
Amherst, MA 01002

MIT Libraries
Technical Reports - Room 14 E-210
Massachusetts Institute of Technology
Cambridge, MA 02139

Document Library L0-206
Woods Hole Oceanographic Institution
Woods Hole, MA 02543

Prof. R. W. Corell
Mechanical Engineering Dept.
Kingsbury Hall
University of New Hampshire
Durham NH 03824

Reprint Custodian
Dept. of Nautical Science
U. S. Merchant Marine Academy
Kings Point, NY 11024

Mr. R. F. Snyder
Ordnance Research Laboratory
Pennsylvania State University
State College, PA 16801

Professor Adrian F. Richards
Marine Geotechnical Laboratory
Lehigh University
Bethlehem, PA 18015

Dr. Houan Yeh
Towne School of Civil & Mechanical Eng.
University of Pennsylvania
Philadelphia, PA 19104

Mr. T. W. Mermel
4540 43rd St., NW
Washington, D.C. 20016

Library of Congress
Science & Technology Division
Washington, DC 20540

W. F. Searle, Jr.
National Academy of Engineering
808 Timber Branch Parkway
Alexandria, VA 22302

Public Documents Department
Wm. R. Perkins Library
Duke University
Durham, NC 27706

Dr R. C. Jordan
Dept of Mechanical Engineering
University of Minnesota
Minneapolis, MN 55455

Dr N. M. Newmark
1114 Civil Engineering Bldg
University of Illinois
Urbana, IL 61801

Professor W. J. Hall
1108 Civil Engineering Bldg
University of Illinois
Urbana, IL 61801

Metz Reference Room
Civil Engineering Dept
B106 Civil Engineering Bldg
University of Illinois
Urbana, IL 61801

Mr. G. A. Sutton
Planning & Development
State Highway Commission
State Office Bldg
Topeka, KS 66612

Acquisition Dept - Serials Section
University of Nebraska Libraries
Lincoln, NE 68508

Robert D. Tent
Undersea Services Division
Fluor Ocean Services Inc
P. O. Drawer 310
Houma, LA 70360

Department of Oceanography
Texas A & M University
College Station, TX 77843

Civil Engineering Dept
Texas A & M University
College Station, TX 77843

R. C. Dehart
Southwest Research Institute
8500 Culebra Road
San Antonio, TX 78228

Wang Civil Engineering Research Facility
P. O. Box 188 - CERF
University Station
University of New Mexico
Albuquerque, NM 87106

Aerospace Corporation
Acquisitions Group
P. O. Box 92957
Los Angeles, CA 90009

TRW Systems
Attn: P. K. Dai R1/2178
1 Space Park
Redondo Beach, CA 90278

Dr F. N. Spiess
Marine Physical Laboratory
Of the Scripps Institution of Oceanography
University of California
San Diego, CA 92152

Engineering Library
Stanford University Libraries
Stanford, CA 94305

Dept of Naval Architecture
College of Engineering
University of California
Berkeley, CA 94720

Engineering Library
University of California
Berkeley, CA 94720

Melvin R. Ramey
Civil Engineering Dept
University of California, Davis
Davis, CA 95616

H. Norby Neilsen
University of Hawaii
Honolulu, HI 96822